*Journal of Engineering Mathematics* **32:** 365–376, 1997.


# Axisymmetric flow in an oil reservoir of finite depth caused by a point sink above an oil-water interface

H. ZHANG[1] and G.C. HOCKING[2]
[1]*Department of Environmental Engineering, University of Western Australia, Nedlands, WA 6907, Australia*
[2]*Department of Mathematics and Statistics, Murdoch University, Murdoch, WA 6150, Australia*

Received 12 June 1995; accepted in revised form 20 January 1997

**Abstract.** The flow of a stratified fluid (*e.g.*, oil/water) withdrawn from a vertically confined porous medium through a point sink is considered. The withdrawal tends to cause the oil-water interface to move upwards. So long as the interface is below the well, the less dense fluid (oil) is pumped into the well without the denser fluid (water) until a critical flow rate is reached. The flow is considered to be axisymmetric, and involves a nonlinear boundary condition along the free surface. A boundary-integral equation method (BIEM) is used to find the interface position for different pumping rates. For small flow rates, a small-parameter expansion is derived and the results are compared with numerical solutions to the problem. There exists a critical withdrawal rate beneath which the water does not break through into the sink, this rate depending on the sink location and bottom geometry.

**Key words:** critical flow rate, boundary-integral-equation method, porous medium.

## 1. Introduction

Most producing oil reservoirs consist of sandstone, limestone or dolomite formations. Within an oil reservoir, fluids are separated into zones by density stratification. The denser fluid occupies the lower position in the trap. As a result, water is often found in a layer below oil [1, 2].

Oil can be pumped from a well situated in an oil layer above an oil-water interface. During pumping, the interface will be drawn upwards to form a cusp as the flow rate is increased, due to the potential distribution established in the two fluids. There exists a critical flow rate, above which the water will enter the well, *e.g.* [3–7] and [8]. Therefore, at steady state, it is of significance to calculate the shape of the coning and thus the critical flow rate for each well position.

Two-dimensional steady sink-like flows near an interface between two immiscible fluids in a porous medium have been studied by means of both the hodograph method and numerical methods. Bear and Dagan [3] used the hodograph method and found a critical flow rate. McCarthy [6] solved this problem by assuming a constant potential boundary across the flow field at some distance from the sink in a lateral-edge-drive model. Recently, Zhang and Hocking [8] employed a model assuming that the flowing layer is confined below by an impermeable boundary, along which it is no longer necessary to satisfy a pressure condition. By assuming the inner edge of this lower boundary to move outward, they observed that the effect of this lower boundary can be gauged. This model could also be considered as a problem in which a layer of oil is trapped between two impermeable rock strata exposed to a small aquifer near the well site. A nonlinear integral-equation solution for this model was solved numerically.

Axisymmetric sink-like flow problems cannot be solved easily with conformal-mapping methods and, in previous work, some approximations were used. Meyer and Garder [9] assumed a critical situation when the cone reaches the bottom of the well and obtained a theoretical flow maximum as a function of the depth of penetration of the well below the top of the oil layer and the thickness of the oil zone at the drainage radius. Muskat and Wyckoff [10] considered the problem of water coning towards a vertical well. It was based on the assumption of horizontal radial flow and disregarded the presence of water coning. In other studies [4, 5], a small perturbation method and a Boundary-Integral Method were applied, and an approximate form for the well-suction pressure in an unconfined oil zone was assumed. In Bruining *et al.*'s research [11], a sharp interface was assumed to exist between the oil and the water, the oil region was assumed to be between the interface and the cap rock and the water in the lower half space of infinite radial extent beneath the interface. The problem was formulated as two singular integral equations and the breakthrough time was found to depend on gravity number and mobility ratio. It was found that no steady critical flow exists. They showed that for this configuration, with unbounded horizontal extent, a two-layer flow will always occur eventually.

The study of withdrawal from water bodies with a free surface is closely related to this problem. A number of papers have considered a series of two-dimensional free-surface flow problems, having in common a submerged source or sink beneath a free surface, *e.g.* [12–15]. These studies have shown that steady flow having a cusped free surface which is horizontal at infinity occurs at a unique Froude number in a fluid of infinite depth, or over a range of Froude numbers for a fluid of finite depth. Some free-surface problems involving three-dimensional, axisymmetric flow into a point sink for infinite and finite depths have been considered by Forbes and Hocking [16, 17]. It was found that solutions with a stagnation point on the free surface occur over an interval of Froude numbers.

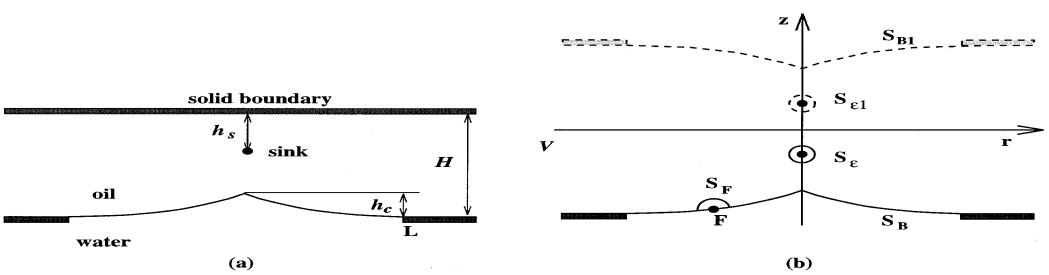


*Figure 1.* (a) The physical plane of an oil reservoir. (b) Volume $V$ and its real bounding surfaces and image bounding surfaces used in the derivation of the integral equation.

In this paper, the flow of two incompressible, immiscible fluids through a porous medium is considered. This problem is of practical importance as it is relevant to oil recovery. An oil reservoir consisting of an oil layer confined above by an impermeable rock strata and below by a water zone and the rock strata is investigated. The rock strata beneath some of the oil layer removes the problem highlighted by Bruining *et al.* [11]. The presence of this boundary makes a steady coning solution possible. The well is represented by a point sink. The physical plane is shown in Figure 1(a).

The boundary-integral equation method (BIEM) is used to solve this problem of axisymmetric flow governed by Laplace's equation. A small-parameter-expansion (SPE) solution for

small flow rate is also derived and the results are compared with those obtained from the numerical computation.

## 2. Problem formulation

We consider a homogeneous and isotropic porous medium of constant permeability $k$ beneath a boundary of impermeable rock. A layer of oil depth $H$ lies above an unbounded region of water, as shown in Figure 1(a). A point sink is now located at a distance, $h_s$, beneath the origin of the Cartesian coordinate system. The inner edge of the lower impermeable boundary is located at $r = r_l$. The coning height is expressed by $h_c$. The sink has strength $Q/4\pi$, so that it produces a total flux $Q$ per unit time.

Since the flow geometry is axisymmetric, we introduce cylindrical polar coordinates $(r, \theta, z)$. Non-dimensional variables are defined. The oil-layer depth, $H$, is used as the reference length. The variables can be nondimensionised as $\Phi^* = \Phi/H$, where $\Phi$ is the velocity potential and $(r^*, z^*) = (r, z)/H$. $Q^* = Q/KH^2$ is used as scaled withdrawal rate, where

$$K = \frac{k}{\mu}\frac{\gamma_w - \gamma_o}{\gamma}.$$

Here $\mu$ is the viscosity of the oil and $\gamma_o$ and $\gamma_w$ are the specific gravity of oil and water, respectively. For brevity, asterisks are dropped in the remainder of this paper.

The incompressible fluid satisfies Laplace's equation [1]

$$\nabla^2\Phi = \Phi_{rr} + \frac{1}{r}\Phi_r + \Phi_{zz} = 0 \tag{2.1}$$

for the velocity potential $\Phi$. The subscripts in (2.1) denote partial differentiation. The velocity potential is singular at the point $S$ (the point sink), where $(r, z) \to (0, -h_s)$, and it becomes infinite according to

$$\Phi \to \frac{1}{4\pi[r^2 + (z + h_s)^2]^{1/2}}, \text{ as } (r, z) \to (0, -h_s).$$

At the unknown free surface location, $z = \zeta(r)$, there are two conditions to be satisfied. The first of these is a kinematical condition, arising from the fact that no flow occurs normal to the surface, and is expressed in the form

$$\Phi_z = \Phi_r\zeta_r, \tag{2.2}$$

on $z = \zeta(r)$. The second condition is a combination of (2.2) and the application of Darcy's law on the interface, *i.e.* $\Phi = K(z + p/\gamma_o)$, where $p$ is the pressure at a point. The lower fluid (water) is stationary, and the entire stationary fluid region is assumed to be at a constant potential. Therefore, matching the pressure in the two fluid regions across each point on the interface, we observe that the condition between a moving fluid (oil, $\gamma_o$) and a stationary fluid (water, $\gamma_w$) in an isotropic medium is [1]

$$Q(\Phi_r^2 + \Phi_z^2) - \Phi_z = 0. \tag{2.3}$$

Within the flow domain, there is no flow across the solid boundaries and interface, a condition which can be described by $q \cdot \mathbf{n} = 0$, where $\mathbf{n}$ is in the direction of the normal, and $q$ is

the specific discharge vector. Solutions are then dependent only on the single parameter of nondimensional withdrawal flow rate $Q$, and the boundary conditions. However, Bruining *et al.* [11] showed that a steady, vertically confined flow was not possible, if the region is of infinite radial extent.

For completeness, we repeat this argument here. If $r \to \infty$, conservation of volume dictates that

$$Q \approx 2\pi r(\zeta - 1)\phi_r. \tag{2.4}$$

The substitution of (2.2) and (2.4) in (2.3) gives

$$\zeta_r^2 - \frac{2\pi r(\zeta - 1)}{Q^2}\zeta_r + 1 = 0. \tag{2.5}$$

When $r \to \infty, \zeta_r$ is small, and (2.5) can be rewritten as:

$$\frac{\mathrm{d}\zeta}{\mathrm{d}r} = \frac{Q^2}{2\pi r(\zeta - 1)}. \tag{2.6}$$

By integration of (2.6), the interface position in the far field can be expressed as

$$\zeta^2 - 2\zeta = \frac{Q^2}{\pi}\log r + C, \quad r \to \infty, \tag{2.7}$$

in which $C$ is a constant. It is clear that $\zeta$ tends to infinity as $r \to \infty$. This means that a stationary flow with a stable interface cannot exist, but it can occur if either the oil-water interface is held fixed at a finite distance $r = r_l$, or the top impermeable boundary is moved to infinity.

In this model, the point sink is present in a domain bounded above by a flat impermeable boundary, and below by a water zone and an impermeable boundary (see Figure 1(a)). Above the solid boundary an image point sink $S_1(r, z) = (0, h_s)$ is assumed and the domain with its boundary is replaced by a fictitious domain (see Figure 1(b)). The dashed lines in Figure 1(b) are the image free surface, so that the zero-flux condition along the solid boundary is satisfied. Therefore, the flow pattern sought and produced by the sink in the real domain is identical to that obtained for the symmetric area when it is part of the fictitious domain.

Let the point $F$ at the fluid interface be a fixed point with cylindrical polar coordinates $(r, \theta, \zeta)$. Define another point $E(\rho, \beta, \mu)$ which is free to move on the interface. We can now derive an integral equation for the velocity potential $\Phi$ at the free surface in which $S_B$ denotes the entire interface with a small circular disk about the point $F$ excluded; $S_{B1}$ is the fictitious free surface, $S_\epsilon$ and $S_{\epsilon 1}$ are small spherical surfaces centred at the sink and the image sink, respectively, and $S_F$ is a small hemispherical surface centred at the point $F$. These surfaces are all displayed in Figure 1(b). If the distance between the points $E$ and $F$ is written as $R_{EF}$, then the function

$$\frac{1}{R_{EF}} = \frac{1}{[r^2 + \rho^2 - 2r\rho\cos(\beta - \theta) + (\zeta - \mu)^2]^{1/2}} \tag{2.8}$$

is harmonic within the volume $V$ shown in Figure 1(b). Therefore, according to Green's theorem, we may write

$$\int\int_{\partial V}\left[\Phi\frac{\partial(\frac{1}{R_{EF}})}{\partial n} - \frac{1}{R_{EF}}\frac{\partial\Phi}{\partial n}\right]\mathrm{d}S = 0. \tag{2.9}$$

The closed boundary surface $\partial V$ consists of

$$\partial V = S_B + S_{B1} + S_\epsilon + S_{\epsilon 1} + S_F. \tag{2.10}$$

Calculation of the contribution of each surface to the integral leads to the desired integral equation for $\Phi$ on the interface,

$$\begin{aligned} 2\pi\Phi(F) \;=\; & \frac{1}{[r^2+(z+h_s)^2]^{1/2}} + \frac{1}{[r^2+(z-h_s)^2]^{1/2}} \\ & - \int\int_{S_B} \Phi(E) \frac{\partial(\frac{1}{R_{EF}})}{\partial n_E}\, \mathrm{d}S_E - \int\int_{S_{B1}} \Phi(E) \frac{\partial(\frac{1}{R_{EF}})}{\partial n_E}\, \mathrm{d}S_E. \end{aligned} \tag{2.11}$$

It is convenient at this stage to remove the singularity in the integrand of the third term of the RHS of (2.11). We may do this in the usual way, by adding and subtracting a term which has the same degree of singularity as that already present in the integrand. Thus, the third term of the RHS of (2.11) is rewritten as

$$\begin{aligned} & \int\int_{S_B} \Phi(E) \frac{\partial(\frac{1}{R_{EF}})}{\partial n_E}\, \mathrm{d}S_E \\ & = \int\int_{S_B} [\Phi(E) - \Phi(F)] \frac{\partial(\frac{1}{R_{EF}})}{\partial n_E}\, \mathrm{d}S_E + \Phi(F) \int\int_{S_B} \frac{\partial(\frac{1}{R_{EF}})}{\partial n_E}\, \mathrm{d}S_E. \end{aligned} \tag{2.12}$$

A Taylor expansion shows that the integrand of the first integral on the right-hand side of (2.12) is now nonsingular, as intended. We may evaluate the second integral in closed form, using a device based upon Gauss's flux theorem. Since the function $1/R_{EF}$ defined in (2.8) is harmonic within the volume $V$ shown in Figure 1(b), we have

$$\int\int_{S_B} \frac{\partial(\frac{1}{R_{EF}})}{\partial n_E}\, \mathrm{d}S_E = 0.$$

The numerical solution of this problem is associated with the surface point $F$ and arclength $s$ along the surface, as described by Forbes and Hocking [16]. We assume that $s = 0$ at $r = 0$, and define $s$ according to

$$\left(\frac{\mathrm{d}r}{\mathrm{d}s}\right)^2 + \left(\frac{\mathrm{d}\zeta}{\mathrm{d}s}\right)^2 = 1. \tag{2.13}$$

A surface velocity potential $\Phi$ is now defined as $\phi(r(s)) = \Phi(r, \zeta(r))$ and it follows that

$$\frac{\mathrm{d}\phi}{\mathrm{d}r} = \Phi_r(r,\zeta) + \Phi_z(r,\zeta)\frac{\mathrm{d}\zeta}{\mathrm{d}r}.$$

The kinematical condition (2.2) and Darcy's law (2.3) are then combined to give a single condition

$$Q\frac{\mathrm{d}\phi}{\mathrm{d}s} - \frac{\mathrm{d}\zeta}{\mathrm{d}s} = 0, \tag{2.14}$$

which is applied along the interface.

After some transformations, the integral equation (2.11) can be rewritten in terms of the arclength as

$$\begin{aligned} 2\pi\phi(s) &= \frac{1}{[r^2+(z+h_s)^2]^{1/2}} + \frac{1}{[r^2+(z-h_s)^2]^{1/2}} \\ &\quad - \int_0^\infty [\phi(\sigma)-\phi(s)]\mathbf{K}(A,B,C,D)\,\mathrm{d}\sigma \\ &\quad - \int_0^\infty \phi(\sigma)\mathbf{K}(A1,B1,C1,D1)\,\mathrm{d}\sigma \end{aligned} \tag{2.15}$$

where the kernel can be written as

$$\mathbf{K}(A,B,C,D) = \frac{-4\rho}{D\sqrt{C+D}}\left[BK\left(\frac{2D}{C+D}\right) + \frac{AD-BC}{C-D}E\left(\frac{2D}{C+D}\right)\right],$$

according to the appendix of [16] and the auxiliary functions are defined as

$$A = r(\sigma)\zeta'(\sigma) - r'(\sigma)[\zeta(\sigma)-\zeta(s)], B = r(s)\zeta'(\sigma)$$

$$C = r^2(\sigma) + r^2(s) + [\zeta(\sigma)-\zeta(s)]^2, D = 2r(s)r(\sigma).$$

$K$ and $E$ are the complete elliptic integrals of the first and second kinds, respectively. These can be approximated by [18],

$$\begin{aligned} K(m) &= (a_0 + a_1m_1 + a_2m_1^2 + a_3m_1^3 + a_4m_1^4) \\ &\quad +(b_0 + b_1m_1 + b_2m_1^2 + b_3m_1^3 + b_4m_1^4)\,\log(1/m_1) + \varepsilon(m), \\ E(m) &= (1 + c_1m_1 + c_2m_1^2 + c_3m_1^3 + c_4m_1^4) \\ &\quad +(d_1m_1 + d_2m_1^2 + d_3m_1^3 + d_4m_1^4)\,\log(1/m_1) + \varepsilon(m), \\ &\quad |\varepsilon(m)| \leqslant 2\times 10^{-8}, \end{aligned} \tag{2.16}$$

where $\varepsilon(m)$ indicates the upper bound of the error for this approximation, and $m = 2D/(C+D)$, $m_1 = 1-m$. All the coefficients in (2.16) are available in [19]. The procedure to calculate $\mathbf{K}(A1,B1,C1,D1)$ is similar to the above. Because the real free surface $\zeta(r)$ is symmetric to the image interface $-\zeta(r)$, we have

$$A1 = -r(\sigma)\zeta'(\sigma) + r'(\sigma)[\zeta(\sigma)+\zeta(s)], B1 = -r(s)\zeta'(\sigma)$$

$$C1 = r^2(\sigma) + r^2(s) + [\zeta(\sigma)+\zeta(s)]^2, D1 = 2r(s)r(\sigma).$$

Therefore, the equations (2.13), (2.14) and (2.15) represent a complete statement of the problem to be solved.

## 3. Small-parameter expansion

We can obtain an asymptotic approximation by assuming a regular expansion in powers of the parameter $Q$,

$$\Phi(r,z) = \Phi_0(r,z) + O(Q) \tag{3.1}$$

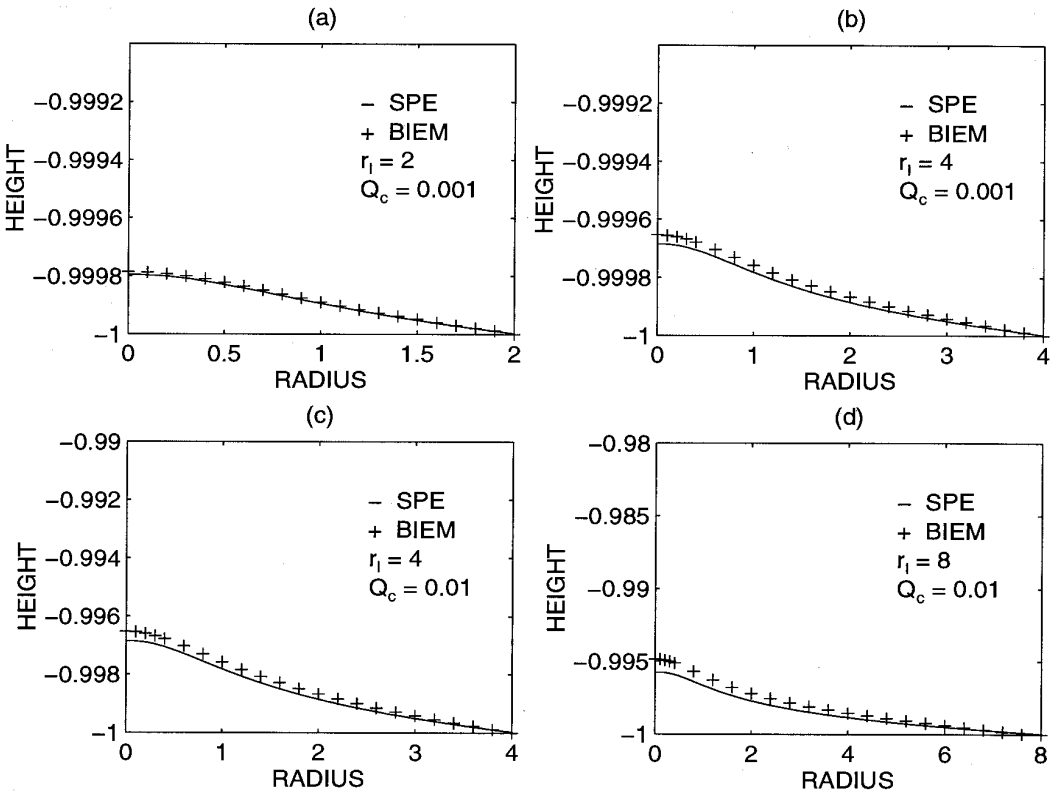


*Figure 2.* The shapes of the free surface calculated with the BIEM compared with the solutions obtained by the SPE.

$$\zeta(r) = -1 + QZ_1(r) + O(Q^2). \tag{3.2}$$

Using the method of images, we arrive at a solution for $\Phi_0$ in the form

$$\Phi_0(r,z) = \frac{1}{4\pi}\sum_{n=0}^{\infty}\frac{1}{[r^2+(z-h_s+2n)^2]^{1/2}} + \frac{1}{[r^2+(z+h_s-2n)^2]^{1/2}}. \tag{3.3}$$

The first-order approximation satisfies the kinematic condition (2.2) and the dynamic free surface condition (2.3) if

$$\Phi_{0r} = -Z_1'(r), \tag{3.4}$$

at $z=-1$. Differentiating (3.3), we have

$$\Phi_{0r} = -\frac{r}{4\pi}\sum_{n=0}^{\infty}\frac{1}{[r^2+(z-h_s+2n)^2]^{3/2}} + \frac{1}{[r^2+(z+h_s-2n)^2]^{3/2}}. \tag{3.5}$$

and then equations (3.4) and (3.5) can be used to obtain $Z_1'(r)$ numerically. Use of the boundary conditions, when $r=r_l, z=-1$, and substitution in (3.2) leads to the first-order approximation for $\zeta(r)$, the shape of the interface.

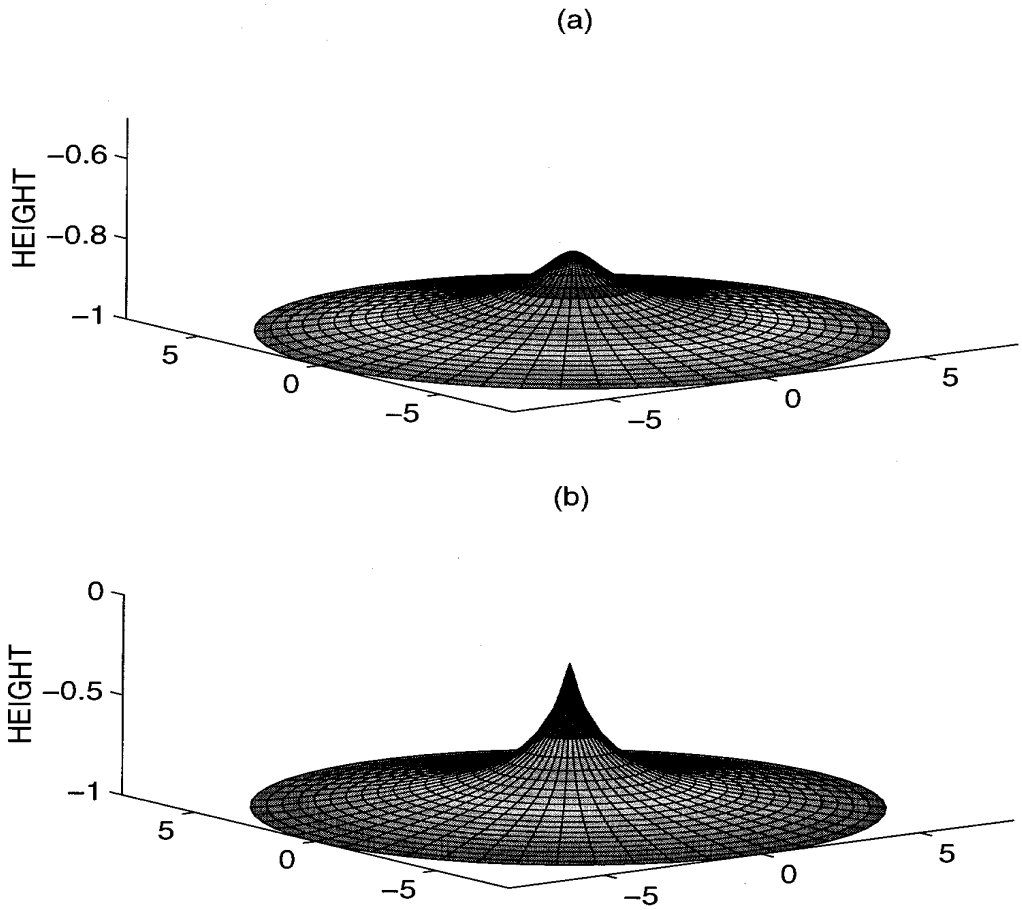


*Figure 3.* The shapes of the free surface calculated with the BIEM with the sink on the upper boundary $h_s = 0{\cdot}0$. (a) Domed shape with the parameter $Q = 0{\cdot}30$. (b) Cusped shape with the critical parameter $Q_c = 0{\cdot}58$.

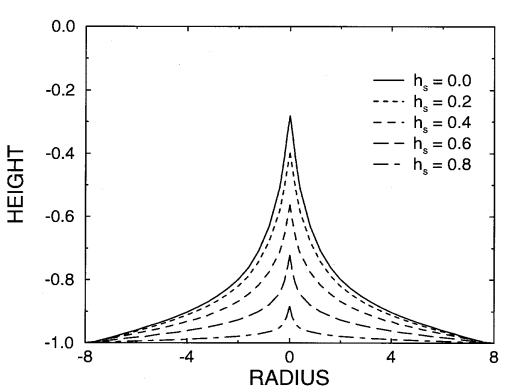


*Figure 4.* The interface in critical cases with the sink at different positions.

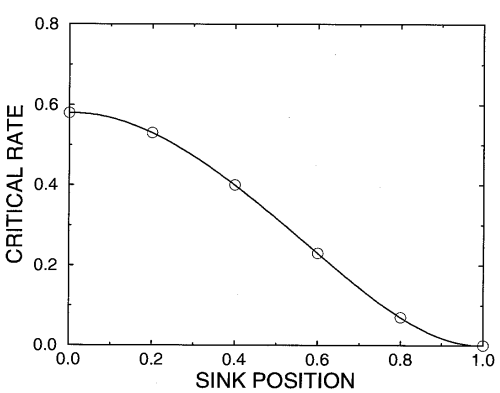


*Figure 5.* The relationship between the critical flow rate the position of the sink for $r_l = 8{\cdot}0$.

## 4. Numerical solution technique

The numerical method for the solution of the governing equations derived in Section 2 is described briefly in this section. The integral terms in Equation (2.15) may be integrated by numerical integration along the real interface. They can be evaluated by Gaussian quadrature. Two different situations are considered separately.

When the base point $F$ does not coincide with either $E_j$ or $E_{j+1}$ $(j = 0, 1, \ldots, N)$, the elliptic integrals have regular behavior. The integral can be expressed over a linear segment as follows:

$$\int_0^\infty [\phi(\sigma) - \phi(s)]\mathbf{K}(A, B, C, D)\,\mathrm{d}\sigma = \sum_{j=0}^{N} \int_{\sigma_j}^{\sigma_{j+1}} [\phi(\sigma) - \phi(s)]\mathbf{K}(A, B, C, D)\,\mathrm{d}\sigma, \quad (4.1)$$

where

$$\int_{\sigma_j}^{\sigma_{j+1}} [\phi(\sigma) - \phi(s)]\mathbf{K}(A, B, C, D)\,\mathrm{d}\sigma$$

$$\approx \frac{1}{2}(\sigma_{j+1} - \sigma) \sum_{i=1}^{M} \omega_i [\phi(\sigma_i) - \phi(s)]\mathbf{K}[A(\sigma_i), B(\sigma_i), C(\sigma_i), D(\sigma_i)]. \quad (4.2)$$

For the linear interpolation of $\phi$ between a pair of consecutive points $E_j$ and $E_{j+1}$ along the interface, we use

$$\phi(\sigma_i) = [(\phi(\sigma_{j+1}) - \phi(\sigma_j))\sigma_i + \sigma_{j+1}\phi(\sigma_j) - \sigma_j\phi(\sigma_{j+1})]/(\sigma_{j+1} - \sigma_j)$$

with

$$\sigma_i = [(\sigma_{j+1} - \sigma_j)\chi_i + \sigma_{j+1} + \sigma_j]/2,$$

where the Gaussian quadrature weights $\omega_i$ and the positions $\chi_i$ are available in Abramowitz and Stegun [18] for different values of the order $M$. In this study, we consider $M = 8$ which gives six-figure accuracy.

When the singular point $F$ is located at either point $E_j$ or $E_{j+1}$, the integrals have an integrable singularity as $\sigma \to \sigma_j$ (or $\sigma_{j+1}$), due to the fact that $K(m)$ has a logarithmic singularity as $m \to 1$. Thus, regular Gaussian quadrature does not give accurate results. To overcome this problem, we rearrange the approximation for $K(m)$ as follows:

$$K(m) = K^*(m) - b_0 \log m_1 \quad (4.3)$$

with

$$K^*(m) = a_0 + \sum_{l=1}^{4} [a_l m_1^l + b_l m_1^l \log(1/m_1)] \quad (4.4)$$

where $K^*(m)$ is a regular function along the segment $\sigma_j \leqslant \sigma \leqslant \sigma_{j+1}$. The other term of function (4.3) has a logarithmic singularity, but it can be evaluated by means of a special Gaussian quadrature, *i.e.*,

$$\int_0^1 f(x) \log x\,\mathrm{d}x = \sum_{i=1}^{M} \omega_i^s f(\chi_i^s), \quad (4.5)$$

where $\omega_i^s$ and $\chi_i^s$ are the special Gaussian-quadrature weights and locations as given by Abramowitz and Stegun [18].

The procedure to calculate the other integral term in (2.15) is similar. Because the point $F$ moves within the surface $S_B$, there are no singularities.

In this problem, the relevant integral equations require only discretization of points along the interface as opposed to other numerical methods where the whole domain must be discretized. For the nonlinear integral equations (2.13), (2.14) and (2.15) the domain $[0, \infty)$ of the independent variable $s$ is split into two parts: $0 \leqslant s \leqslant s_N (s_0 = 0, s_1, \ldots, s_N)$ and $s_N \leqslant s \leqslant \infty$. In this problem, the solution domain extends to infinity, the calculation should be extended far enough so that the artificial boundaries introduced by the method do not seriously affect the solution.

In summary, the numerical procedure is as follows. An initial guess is made for the unknown values of the derivatives of the velocity potential $(\phi_0', \phi_1', \ldots, \phi_N')$ and these will eventually be updated by a Newtonian iteration scheme. All the other dependent variables are computed on the basis of this guess. The surface condition (2.14) yields the derivatives of the surface elevation $\zeta_0', \zeta_1', \ldots, \zeta_N'$, and (2.13) provides an immediate means for the calculation of $s_0, s_1, \ldots, s_N$. We obtain the values of $(\phi_0, \phi_1, \ldots, \phi_N)$, $(\zeta_0, \zeta_1, \ldots, \zeta_N)$ and $(s_0, s_1, \ldots, s_N)$ by integrating the values for $\phi', \zeta'$ and $r'$ using Gaussian quadrature, respectively. Notice that for the first point $s_0 = 0, r_0 = 0$ and $\zeta_N = -1$ are applied to obtain the interface position.

The initial estimate for the values of the derivative of the velocity potential $\phi$ is now updated iteratively with Newton's method to enforce the conditions (2.15) at each of the mesh points.

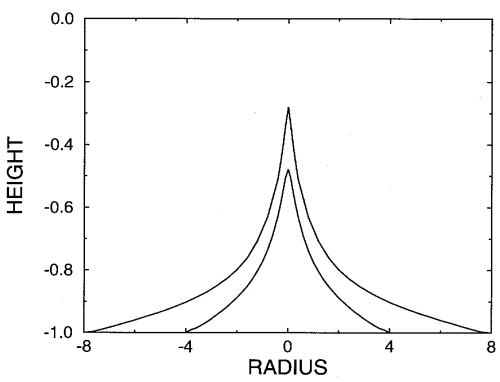


*Figure 6*. The free surfaces in critical cases with the same sink positions $h_s = 0{\cdot}0$ and different bottom boundary locations.

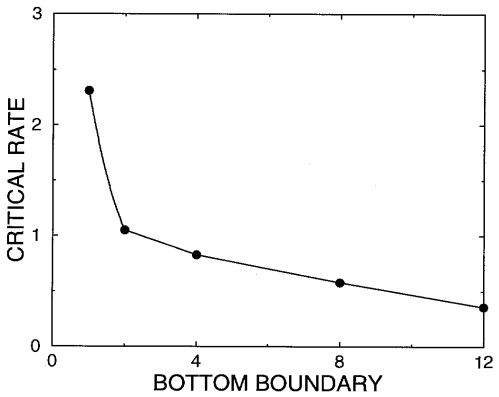


*Figure 7*. The relationship between the critical flow rate and the position of the bottom boundary.

## 5. Discussion of the results

The solutions of this problem depend on the parameter $Q$, the sink position $h_s$ and the bottom boundary location $r_l$. When the flow rate $Q$ is quite small, we calculate the solution, using a small-parameter expansion and using a BIEM. Figure 2 shows that the two solutions are in good agreement, having a stagnation point directly under the sink.

As the flow rate $Q$ increases, the interface is drawn up from a domed shape until the critical rate $Q_c$ is reached when a cusp shape forms. We have found the critical value of $Q_c$

by increasing $Q$ to find at what maximum value a converged cone shape is possible. Figure 3 shows the shape of the interface for two flow rates, where the sink is on the top boundary $h_s = 0{\cdot}0$ and the bottom boundary $r_l = 8{\cdot}0$.

The behavior of the critical flow is the most important aspect of this work, because that is when the water breaks through into the sink. This has a profound effect on the quality and quantity of oil production. When the flow rate $Q > Q_c$, the numerical model diverges, and a stable solution is not obtained.

The location of the sink plays an important role in the shape of the interface. When the bottom boundary is fixed, and the vertical height $h_s$ between the well and the top boundary increases, the critical values of the parameter $Q_c$ decrease and the coning height declines as well. Figure 4 shows the interface profiles in these critical case. In Figure 5, the relationship between sink position and critical rate is shown. When the sink is located at the top boundary $Q_c$ is maximal, and when the sink is moved close to the bottom boundary, $Q_c$ tends to zero.

The bottom boundary also affects the critical flow rate. If the sink position is fixed and the bottom boundary is moved outwards horizontally, the coning height $h_c$ increases, as shown in Figure 6, but the value of $Q_c$ will decrease as shown in Figure 7. It is clear that $Q_c \to 0$ as $r_l \to \infty$, and $Q_c \to \infty$ as $r_l \to 0$. This work confirms the conclusions of Bruining *et al.* [11], who showed that if the domain is unbounded horizontally, supercritical, two-layer flow will always eventuate. It does add to this in that it shows that a critical steady solution is possible if the lower fluid is of limited horizontal extent.

The results of this study of the axisymmetric flow into a point sink from an oil zone of finite depth has much in common with two-dimensional flow into a line sink, as reported in [8] and [20]. In both cases, a stationary situation with an equilibrium cone below the sink which satisfies $h_c < h_s$ and $r_l(x_l) \to \infty$ cannot exist, while $Q_c \to \infty$ as $r_l \to 0$. In order to obtain high efficiency of pumping, Zhang, Barry and Hocking [21] examined a supercritical flow rate, pulsed pumping strategy. They found that the efficiency of the withdrawal can be improved if the pumping and rebound cycles are suitably chosen.

## 6. Conclusion

The shape of an oil-water interface caused by flow into a point sink in an oil reservoir which is confined above by an impermeable rock strata and below by a water zone and a rock strata, has been investigated by the BIEM. It was found that there is an upper limit to the flow rate, above which the water will also enter the sink. At the critical flow rate the interface has a vertical cusp shape. The locations of the well and the bottom rock strata influence the shaping of the interface. These solutions provide us with useful information for choosing optimal withdrawal rates in a variety of circumstances.

## Acknowledgments

The authors would like to thank D.A. Barry for comments on a draft of this paper, whose suggestions led to substantial improvements in the final version, and the anonymous referees whose suggestions resulted in a significant improvement in this work.

## References

1. J. Bear, *Dynamics of fluids in porous media*. New York: American Elsevier (1972) 764 pp.
2. C. Yih, *Stratified flows*. New York: Academic Press (1980) 418 pp.

3. J. Bear and G. Dagan, Some exact solutions of interface problems by means of the hodograph method. *J. Geophys. Res.* 69 (1964) 1563–1572.
4. J.R. Blake and Kucera, Coning in oil reservoirs. *Math. Scientist* 13 (1988) 36–47.
5. S.K. Lucas, J.R. Blake and A. Kucera, A boundary-integral method applied to water coning in oil reservoirs. *J. Austral. Math. Soc. Ser. B* 32 (1991) 261–283.
6. J.F. McCarthy, Gas and water cresting towards horizontal wells. *J. Austral. Math. Soc. Ser. B* 35 (1993) 174–197.
7. J.F. McCarthy, Improved model of water cresting. *J. Austral. Math. Soc. Ser. B* 35 (1993) 207–222.
8. H. Zhang and G.C. Hocking, Withdrawal of layered fluid through a line sink in a porous medium. *J. Austral. Math. Soc. Soc. Ser. B* (in press).
9. H.I. Meyer and A.O. Garder, Mechanics of two immisicible fluids in porous media. *J. Appl. Phys.* 25 (1954) 1400–1406.
10. M. Muskat and R.B. Wyckoff, An approximate theory of water coning in oil production. *Trans. AIME* 114 (1935) 144–163.
11. J. Bruining, C.J. Van Duijn and R.J. Schotting, Simulation of coning in bottom water-driven reservoirs, *Transp. Porous Media* 6 (1991) 35–69.
12. I.L. Collings, Two infinite-froude-number cusped free-surface due to a submerged line source or sink. *J. Austral. Math. Soc. Ser. B* 28 (1986) 260–270.
13. G.C. Hocking, Critical withdrawal from a two-layer fluid through a line sink. *J. Eng. Math.* 25 (1991) 1–11.
14. G.C. Hocking, Subcritical free-surface flow caused by a line source in a fluid of finite-depth. *J. Eng. Math.* 26 (1992) 455–466.
15. E.O. Tuck and J.-M. Vanden Broeck, A cusp-like free-surface flow due to a submerged source or sink. *J. Austral. Math. Soc. Ser. B* 25 (1984) 443–450.
16. L. Forbes and G.C. Hocking, Flow caused by a point sink in a fluid having a free surface. *J. Austral. Math. Soc. Ser. B* 32 (1990) 231–249.
17. L. Forbes, G.C. Hocking and G.A. Chandler, A note on withdrawal through a point sink in fluid of finite depth[1]. *J. Austral. Math. Soc. Ser. B* (in press).
18. M. Abramowitz and I.A. Stegun (eds.), *Handbook of mathematical functions*. New York: Dover Publications (1965) 1046 pp.
19. J.A. Liggett and and P.L-F. Liu, *The boundary integral equation method for porous media flow*, London: George Allen & Unwin (1983) 255 pp.
20. H. Zhang, G.C. Hocking and D.A. Barry, An analytical solution for critical withdrawal of layered fluid through a line sink in a porous medium. *J. Austral. Math. Soc. Ser. B* (in press).
21. H. Zhang, D.A. Barry and G.C. Hocking, Fluid response in the vicinity of a recovery well pumped at a supercritical flow rate. *Proceedings of American Geophysical Union 16th Annual Hydrology Days* (1996) 547–557.